Pictorial Essay

J Korean Soc Radiol 2019;80(2):283-293
https://doi.org/10.3348/jksr.2019.80.2.283
pISSN 1738-2637 / eISSN 2288-2928

대한영상의학회지

Superficially Palpable Masses of the Scalp and Face: A Pictorial Essay

두피 및 얼굴의 표재성 촉지병변: 임상화보

Hyoung Seop Kim, MD, Jin Kyung An, MD*, Jeong Joo Woo, MD, Ra Gyoung Yoon, MD

Department of Radiology, Nowon Eulji Medical Center, Eulji University School of Medicine, Seoul, Korea

Received June 25, 2018
Revised July 30, 2018
Accepted August 4, 2018

***Corresponding author**
Jin Kyung An, MD
Department of Radiology,
Nowon Eulji Medical Center,
Eulji University
School of Medicine,
68 Hangeulbiseok-ro, Nowon-gu,
Seoul 01830, Korea.

Tel 82-2-970-8290
Fax 82-2-970-8346
E-mail jkan0831@eulji.ac.kr

ORCID iDs
Jin Kyung An
https://orcid.org/0000-0003-1086-426X
Hyoung Seop Kim
https://orcid.org/0000-0001-7350-6318

Palpable lesions of the scalp and face are common in clinical practice. They are usually small and benign, and the lesions tend to be treated simply according to the clinical symptoms. However, radiologic evaluation is often performed to determine the exact type and location of a lesion to ensure appropriate management. Ultrasonography is useful as a primary and definitive modality for evaluating small superficial lesions. CT and MRI are better for characterizing soft tissue features and provide superior soft tissue resolution. This article discusses various lesions and their imaging findings of the scalp and face that may present as superficially palpable masses.

Index terms Scalp; Face; Palpation; Ultrasonography; Computed Tomography, X-Ray; Magnetic Resonance Imaging

INTRODUCTION

Palpable lesions of the head and neck are common in clinical practice. Many different lesions may be observed from the scalp to the face and neck, and may be classified into various categories according to their location and histological characteristics. According to the World Health Organization classifications, published in 2017, head and neck tumors are grouped into 10 major categories based on location (1). Some of these tumors may present as palpable lesions, but they may also manifest signs other than palpable lesions depending on their locations. Palpable lesions are often recognized early and may motivate patients to seek medical help. Many studies have focused on head and neck masses; however, there are few studies focusing on scalp or face masses, which are frequently encountered in clinical settings.

Radiologic evaluation is essential for the diagnosis and treatment of tumors. Ultrasonography (US) is often used as the primary imaging modality for palpable lesions and

may help characterize cystic or vascular masses. CT is useful for the evaluation of calcified lesions, tissue discrimination, spatial resolution, staging, mass effect, and treatment planning. MRI is superior in discriminating between tumor and normal tissue (2). It is important for the radiologist to be familiar with various types of lesions and their findings on imaging.

The purpose of this article is to illustrate the various lesions of the scalp and face that may present as palpable lesions. The lesions described here were selected according to frequency of occurrence, which was determined by analyzing lesions in patients who underwent radiologic evaluation for superficially palpable masses in our hospital. The lesions have been described in the following order according to their origin: cutaneous layer, subcutaneous layer, muscle layer, bone layer, and the parotid gland.

CUTANEOUS AND SUBCUTANEOUS LAYER

EPIDERMAL CYST

Epidermal cysts, also known as epidermoid cysts or epidermal inclusion cysts, are benign cutaneous or subcutaneous lesions lined with stratified squamous epithelium and filled with keratin debris (3-5). Epidermal cysts may form when hair follicles become obstructed. They may also arise from traumatic or surgical implantation of the epidermis resulting in lesions of non-follicular areas, hence the synonym epidermal inclusion cyst. They grow slowly and may reach several centimeters in diameter. Cutaneous dermoid cysts are different lesions from epidermal cysts in that they contain normal cutaneous structures such as hair, sebaceous lobules, eccrine glands, apocrine glands, and/or smooth muscle. The sebaceous gland content is responsible for the fatty element of the lesions. They are usually 1–4 cm in diameter and commonly located around the eyes (5-9). On US, with or without through transmission, epidermal cysts appear as well-circumscribed, oval, hypo- or hyperechoic masses (Fig. 1A) (4, 10-14). They also show a lack of internal vascularity, which can differentiate them from other solid masses (14). On CT, these lesions have attenuation similar to that of skeletal muscle (Fig. 1B) (3). On MRI, they appear as well-defined masses with high T2 signal intensity and high or iso T1 signal intensity compared to underlying muscle (Fig. 1C, D) (8, 13-15).

PILOMATRICOMA

A pilomatricoma, or calcifying epithelioma of Malherbe, is a tumor arising from primitive cells that differentiate into the hair matrix. They usually occur as solitary lesions; the most common sites are the head, neck, and upper extremities. Tumors vary in diameter from 0.5–3.0 cm. They frequently present as firm, deep-seated nodules located in the lower dermis (3, 16, 17). Early lesions are usually cystic, consisting of basaloid cells lining the cystic cavity which are contiguous with eosinophilic shadow cells admixed with keratin in the center of the lesion. Older pilomatricoma lesions become solid, with prominent shadow cells, keratin debris, secondary multinucleated giant cells, and dystrophic calcifications (16). Calcifications are seen in about 85% of lesions (3, 17). On US, the lesions appear as subcutaneous hypoechoic masses, with internal echogenic foci, hypoechoic rims, or posterior acoustic shadowing from internal calcifications (Fig. 2A). They may show mild to moderate vascularity on color Doppler imaging (18, 19). CT imaging shows a calcified nodule in the subcutaneous

Fig. 1. Epidermal cysts on ultrasonography, CT, and MRI.
A. Sonogram shows an oval shaped, heterogeneous, hypoechoic mass with posterior acoustic enhancement arising from the dermal layer.
B. Post-contrast CT scans show a well-defined, oval, hypo-attenuated mass in the left cheek abutting into and pushing the overlying skin. There is no enhancement on the post-contrast study (arrow).
C, D. T1 (C) and T2 (D)-weighted axial MRI show a well circumscribed oval mass with high signal intensity in the right supraorbital area (arrows).

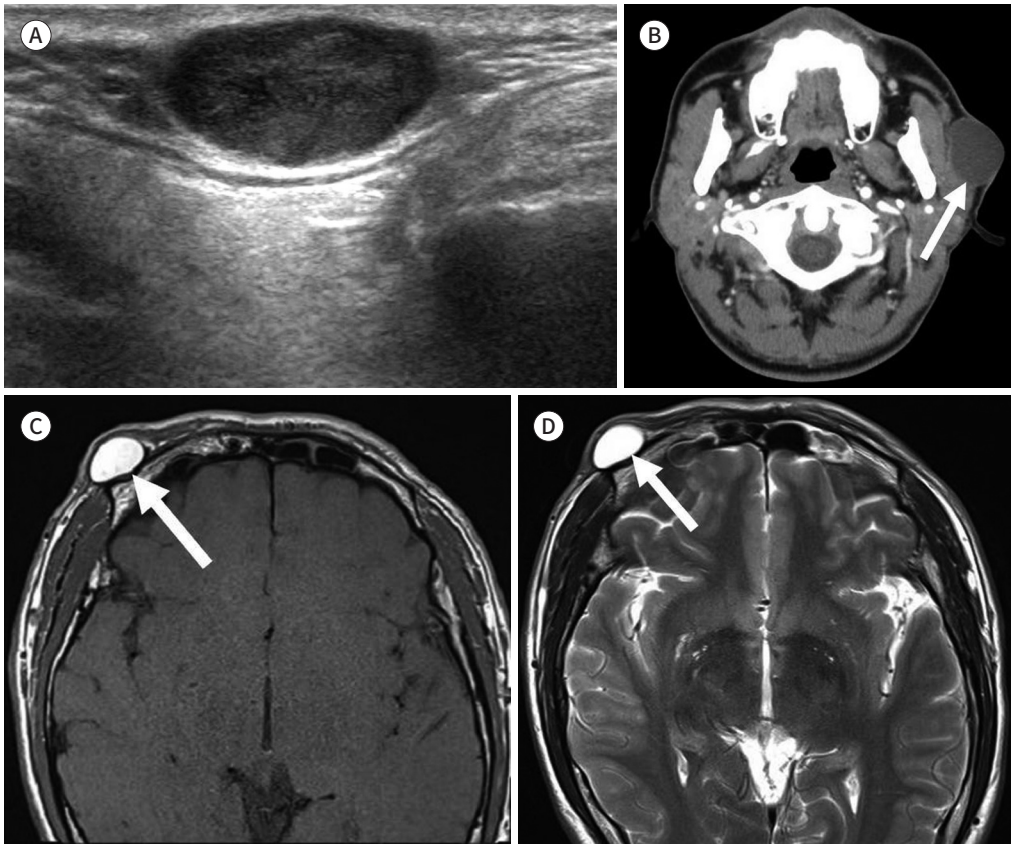

layer (Fig. 2B).

HEMANGIOMA

Hemangiomas are benign vascular neoplasms which grow by endothelial cell hyperplasia. They should be differentiated from vascular malformations, which are localized defects of vascular morphogenesis (20-22). Up to 70% of hemangiomas are visible at birth and 87% are diagnosed by 1 month of age (23). They occur most frequently in the head and neck region (60%), followed by the trunk (25%) and the extremities (15%) (21, 22). Hemangiomas are classified as either infantile or congenital hemangiomas (20-22, 24). Infantile hemangiomas develop shortly after birth and undergo a rapid proliferative phase during the first 6–12 months of life followed by spontaneous regression. The lesions usually resolve between 5 and 9 years of age. Congenital hemangiomas present as fully developed lesions at birth which may rapidly involute during the first year of life; some lesions may never involute. On US, hemangiomas show either poorly defined or well-defined hypoechoic masses with heterogeneous echotexture from multiple cystic spaces. They may display high vascular flow

on color Doppler imaging, particularly in the proliferative phase (Fig. 3). On CT, they are isoattenuating relative to muscle on non-contrast scans and show avid enhancement on contrast-enhanced scans, particularly in the proliferative phase. On MRI, they are isointense to slightly hyperintense on T1-weight imaging, hyperintense on T2-weighted imaging,

Fig. 2. Pilomatricomas on ultrasonography and CT.
A. Sonogram shows three different pilomatricomas: a well-defined oval isoechoic mass with internal hyperechoic spots and small pit (arrowhead) (upper), a parallel heterogeneously hypoechoic mass with internal calcifications (middle), a dense calcified lesion with strong posterior shadowing (lower).
B. Pre-contrast CT scan shows a small, oval, calcified lesion in the subcutaneous layer of the right cheek (arrow).

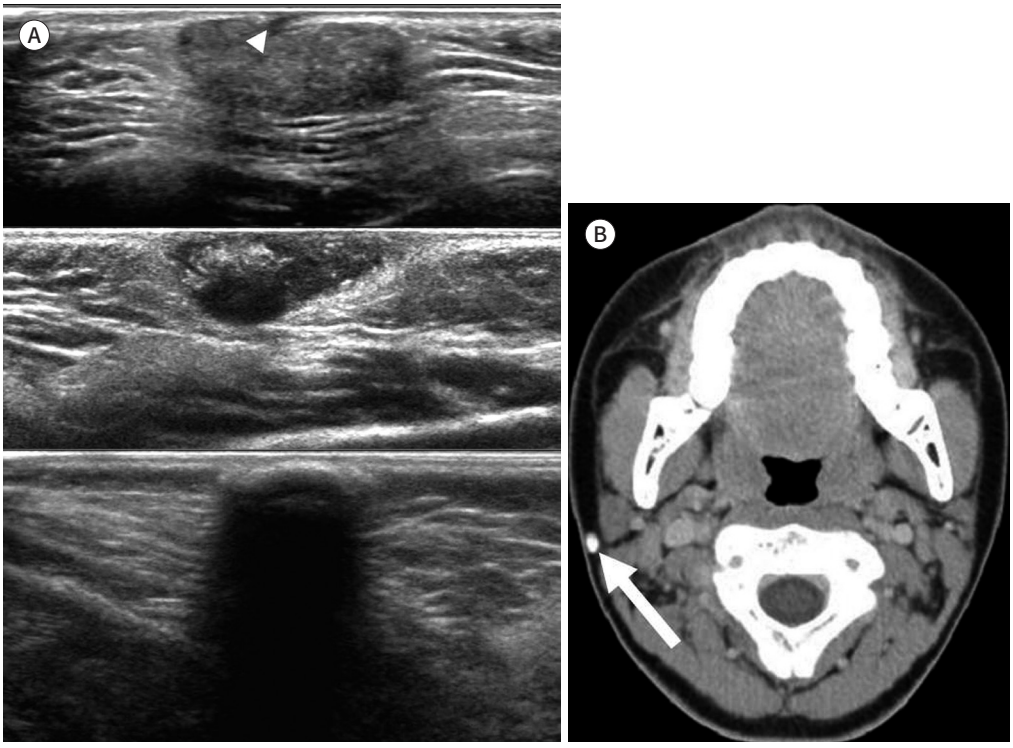

Fig. 3. Hemangioma in a 37-year-old man.
A. Sonogram shows an ill-defined, irregular, heterogeneous, hypoechoic mass involving the cutaneous layer of the left lower eyelid.
B. The mass shows inner vascularity on a color Doppler study.

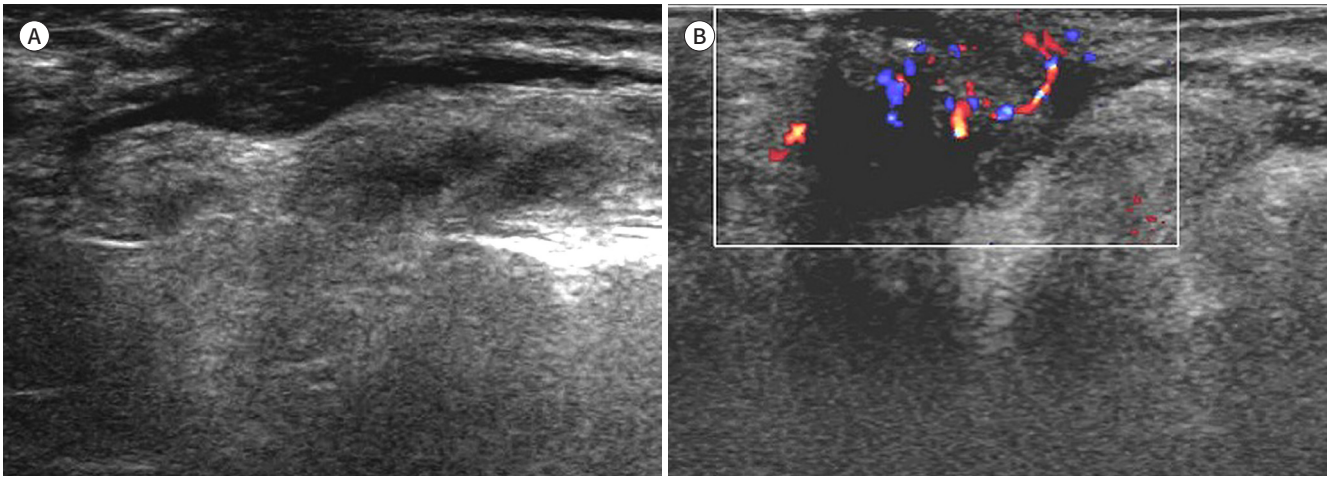

and demonstrate avid contrast enhancement (23, 24).

BRANCHIAL CLEFT CYST

Branchial cleft anomalies arise from the incomplete obliteration of a branchial tract, resulting in a cyst, sinus, or fistulous track (25). They are the second common congenital head and neck lesions in children (26, 27). Second branchial cleft anomalies account for 95% of all branchial cleft lesions and typically result in cyst formation. They are often located close to the anterior border of the sternocleidomastoid muscle. First branchial cleft anomalies are relatively less common and are located close to the parotid gland. US of a typical branchial cleft cyst shows a well-defined, unilocular, anechoic lesion without internal debris or vascularity. Infection or hemorrhage may result in thick walls, internal debris, and septa (Fig. 4A). CT imaging shows sharp margins, fluid density, and thin walls (Fig. 4B, C). Cyst wall thickness and enhancement vary with the degree of inflammation. MRI demonstrates the cystic property of high signal intensity on T2-weighted imaging, but T1 signal intensity may range from low to high with variation in the proteinaceous contents of the cyst (26, 27).

SUBCUTANEOUS AND MUSCLE LAYER

LIPOMA

Lipomas are the most common mesenchymal neoplasms and consist of mature fat cells. Approximately 25% of lipomas occur in the head and neck, primarily in the subcutaneous layer of the posterior neck (28). Most are well-defined encapsulated masses found in the subcutaneous layer or between muscles and other connective tissue structures. There are a number of lipoma variants. Fibrolipomas are rich in fibrous connective tissue, while angiolipomas are characterized by prominent thin-walled blood vessels. Non-adipose areas show low signal intensity on T1-weighted images and high signal intensity on T2-weighted images. They show a variable enhancement pattern following intravenous contrast administration.

Fig. 4. Branchial cleft cysts on ultrasonography and CT.
A. Sonogram shows an oval hypoechoic mass with internal debris and posterior acoustic enhancement in the subcutaneous layer.
B. Pre-contrast CT scan shows a well-defined oval mass in the cutaneous layer of the right preauricular area. The mass shows slightly low attenuation compared to muscle (arrow).
C. Post-contrast CT scan shows no enhancement of the mass (arrow).

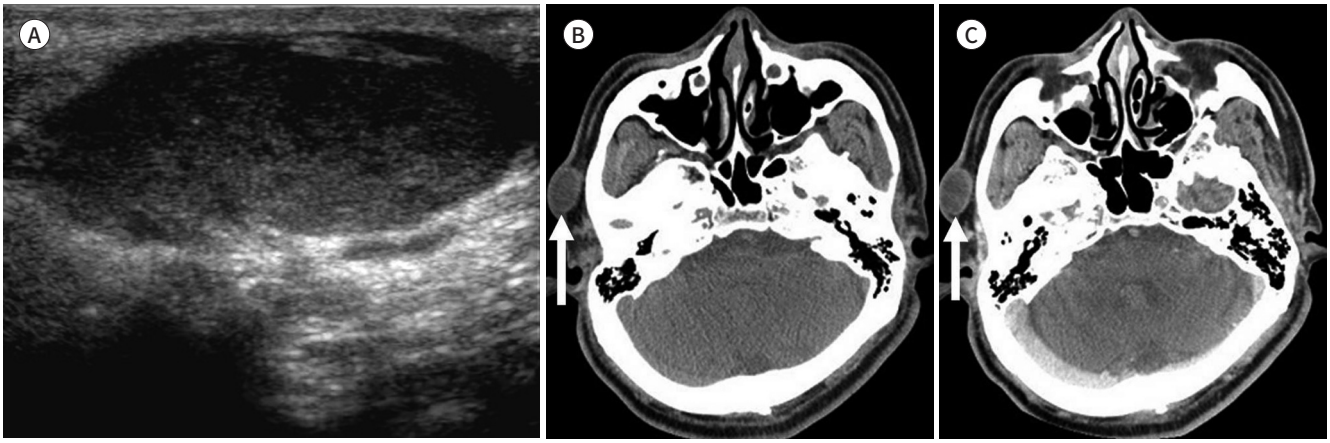

Myxolipomas are lipomas with degenerative changes and a prominent mucoid area. Myolipomas contain variable amounts of benign smooth muscle and mature adipose tissue (28, 29). On US, lipomas are typically homogeneous and hyperechoic relative to the adjacent soft tissue. They may contain echogenic lines parallel to the skin surface (Fig. 5A, B). They show characteristic low attenuation on CT (Fig. 5C) and T1 high signal intensity on MRI.

BONE LAYER

OSTEOMA

Osteomas are the most common benign neoplasms of the skull and are composed of variable proportions of compact and trabecular bone (30-33). They tend to grow along the outer table of the skull, primarily in the frontal or parietal bones, and are either sessile or pedunculated (31). Osteomas are benign, painless, slow-growing tumors (32). On US, bony protrusion can be identified with shadowing (Fig. 6A). Osteomas are typically juxtacortical, well-defined, round or oval sclerotic lesions on CT (Fig. 6B). They do not have soft tissue components and do not show enhancement. On MRI, these lesions are hypointense on T1-weighted imaging and have variable signal intensity on T2-weighted imaging, depending on the proportions

Fig. 5. Lipomas on ultrasonography and CT.
A. Sonogram shows an approximately 2 cm lentiform, striated, hyperechoic mass in the muscle layer.
B. Another elliptical and striated hyperechoic mass is located in the sub-galeal layer of the right temporal area, which was confirmed to be a fibrolipoma.
C. Post-contrast CT scan shows a circumscribed oval fatty mass in the muscle layer of the right temporal area (arrow).

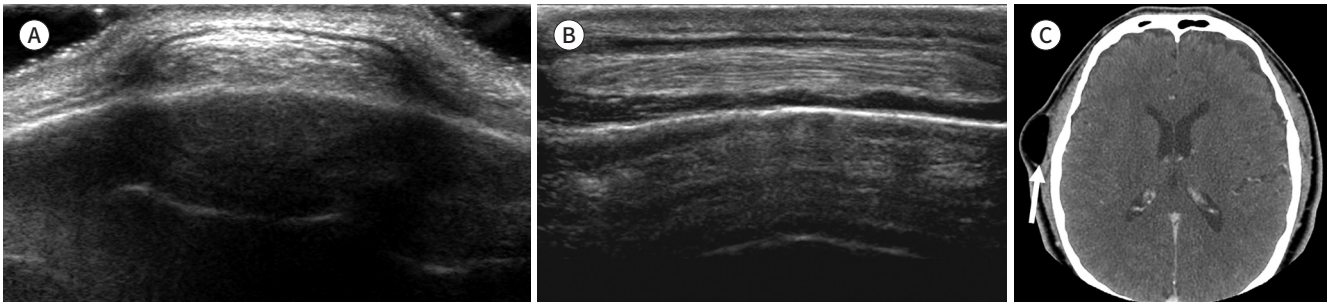

Fig. 6. Osteomas on ultrasonography and CT.
A. Sonogram shows a protruding bony mass with posterior shadowing on the forehead.
B. Pre-contrast CT scan demonstrates a circumscribed bony mass in the frontal area of the skull (arrow).

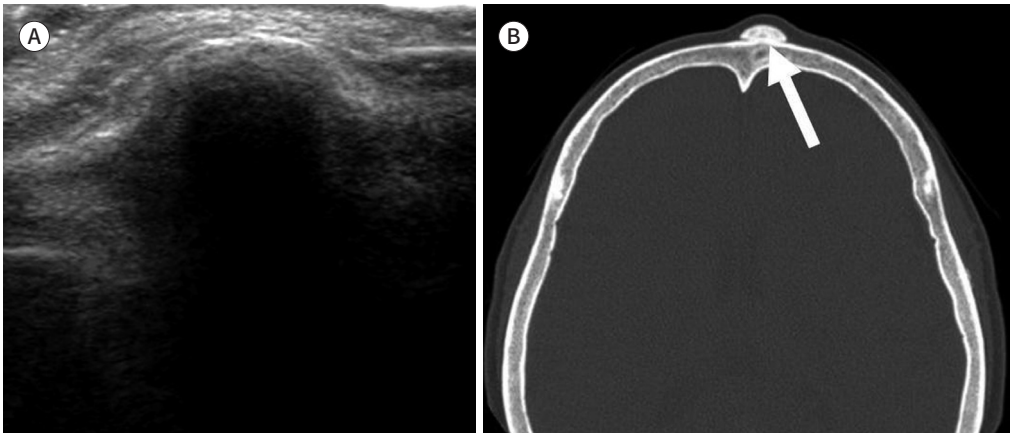

of compact and cancellous bone (30–32).

PAROTID GLAND

PLEOMORPHIC ADENOMAS

Pleomorphic adenomas are the most common benign salivary gland tumors in adults. They predominantly affect the superficial lobe of the parotid gland. Pleomorphic adenomas originate from epithelial and connective tissue (34-36). On US, pleomorphic adenomas appear as heterogeneous solid masses (Fig. 7A). On CT and MRI, smaller tumors are more homogeneous and well-defined with strong enhancement, whereas larger tumors tend to show a lobulated contour and are more heterogeneous, including necrotic and hemorrhagic areas (Fig. 7B-E) (34–36).

WARTHIN'S TUMOR

Warthin's tumors are the second most common benign salivary gland tumors and are located primarily on the lower pole of the parotid gland. They usually present as asymptomatic, slow growing, and well-encapsulated masses. These tumors consist of an oncocytic epithelial cell component, which develops cysts and papillary projections, and a variable amount of lymphoid tissue (34-36). Warthin's tumors present as well-circumscribed partly cystic and partly solid lesions. US images of Warthin's tumors show heterogeneous solid masses or complex cystic lesions. They may show variable vascularity on a color Doppler study (Fig. 8A, B). They tend to show isoattenuation on pre-contrast CT images and strong early enhancement patterns after contrast injection (Fig. 8C, D) (34-36).

MUCOEPIDERMOID CARCINOMA

Mucoepidermoid carcinomas are malignant salivary gland neoplasms arising from ductal epithelium; 50% of these tumors arise from the parotid gland. They are pathologically classified as low, intermediate, or high-grade and imaging features depend on the histological type. Low-grade lesions are well circumscribed, whereas high-grade lesions tend to have poorly defined margins and infiltrate surrounding tissues. Low to intermediate signal inten-

Fig. 7. Pleomorphic adenomas on ultrasonography, CT, and MRI.
A. Sonogram shows a circumscribed, lobular, heterogeneous, hypoechoic mass deep in the left parotid gland.
B. Pre-contrast CT scan shows a slightly low attenuated mass in the left parotid gland (arrow).
C. Post-contrast CT scan shows a well-defined lobulated mass with heterogeneous enhancement in the left parotid gland (arrow).
D. Another mass of the right parotid gland shows a well-defined lobular shape with intermediate signal intensity on T1-weighted MRI (arrow).
E. Post-contrast T1-weighted fat saturated axial MRI shows heterogeneous strong enhancement of the mass (arrow).

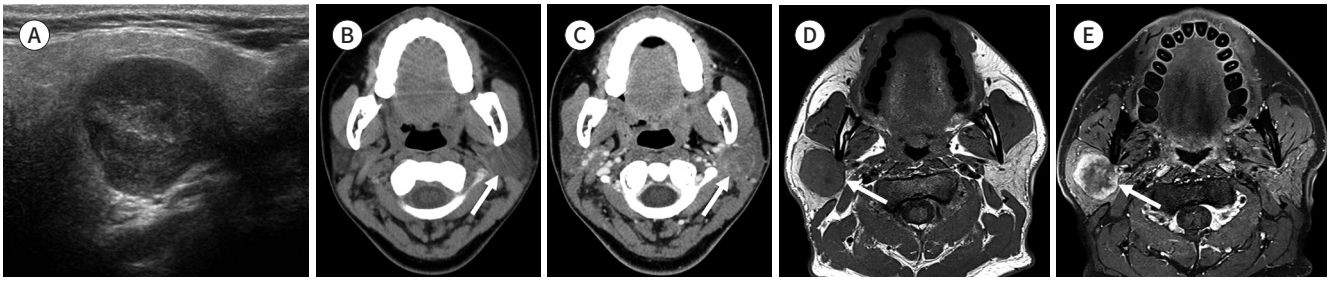

Fig. 8. Warthin's tumor in a 81-year-old-woman.
A. Sonogram shows a well-circumscribed, heterogeneous, hypoechoic mass in the left parotid gland with internal anechoic portions.
B. Color Doppler study shows increased inner and peripheral blood flow of the mass.
C. Pre-contrast axial CT scan shows a well-defined round mass in the left parotid gland with isoattenuation compared to adjacent muscle (arrow).
D. Post-contrast axial CT scan shows heterogeneous internal enhancement with irregular non-enhancing portions (arrow).

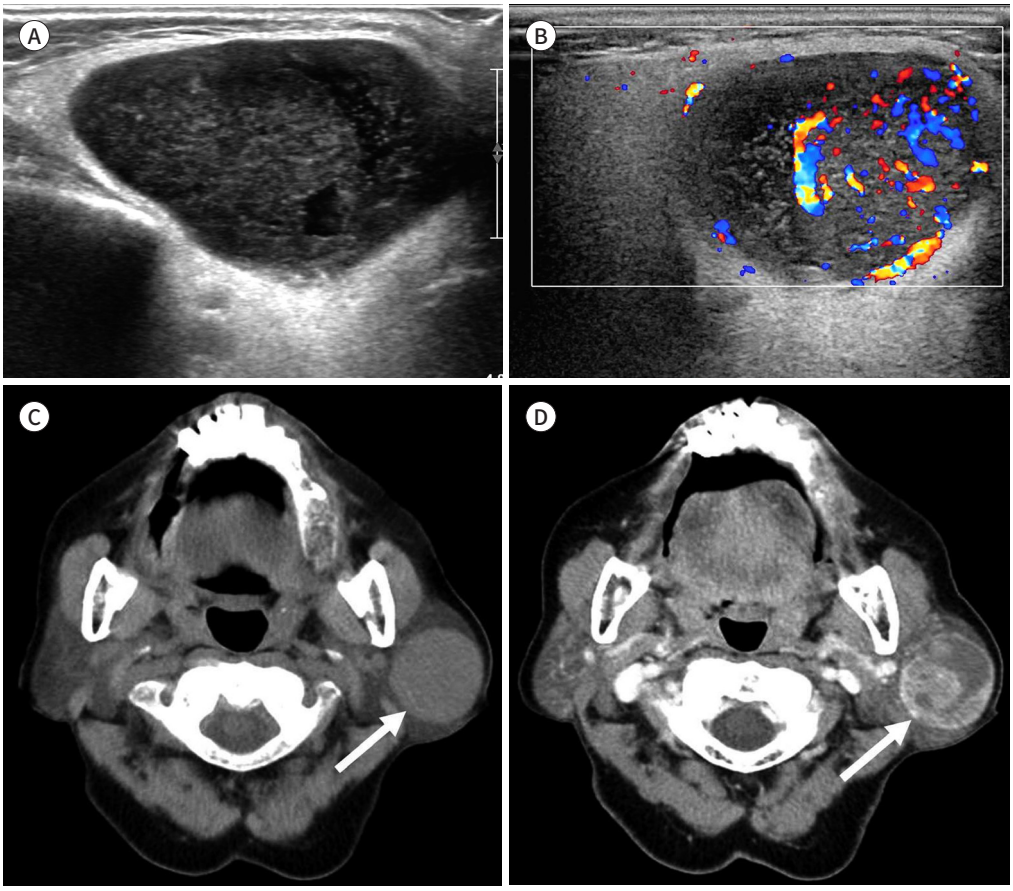

sity may be observed on T1- and T2-weighted images (34-37). On US, mucoepidermoid carcinomas show an ill-defined, irregular, complex echoic mass (Fig. 9).

CARCINOMA EX PLEOMORPHIC ADENOMA

Carcinoma ex pleomorphic adenomas arise from malignant changes of a benign pleomorphic adenoma or as a malignant tumor in a patient with a surgical history of a pleomorphic adenoma. The rapid growth of a pre-existing tumor with associated pain, facial nerve paralysis, and skin fixation are suggestive of malignant transformation. An irregular shape, infiltrative margin, and low T2 signal intensity may be observed in carcinoma ex pleomorphic adenomas (34-36, 38). On MRI, it shows intermediate signal intensity on T1-weighted imaging, low to high signal intensity on T2-weighted imaging, and heterogeneous enhancement on the post-contrast study (Fig. 10).

Fig. 9. Mucoepidermoid carcinoma in a 65-year-old-woman.
A. Sonogram shows an approximately 1.5 cm, oval, heterogeneous, hypoechoic mass with an irregular margin in the superficial lobe of the left parotid gland.
B. Some peripheral blood flow is seen on a color Doppler study.

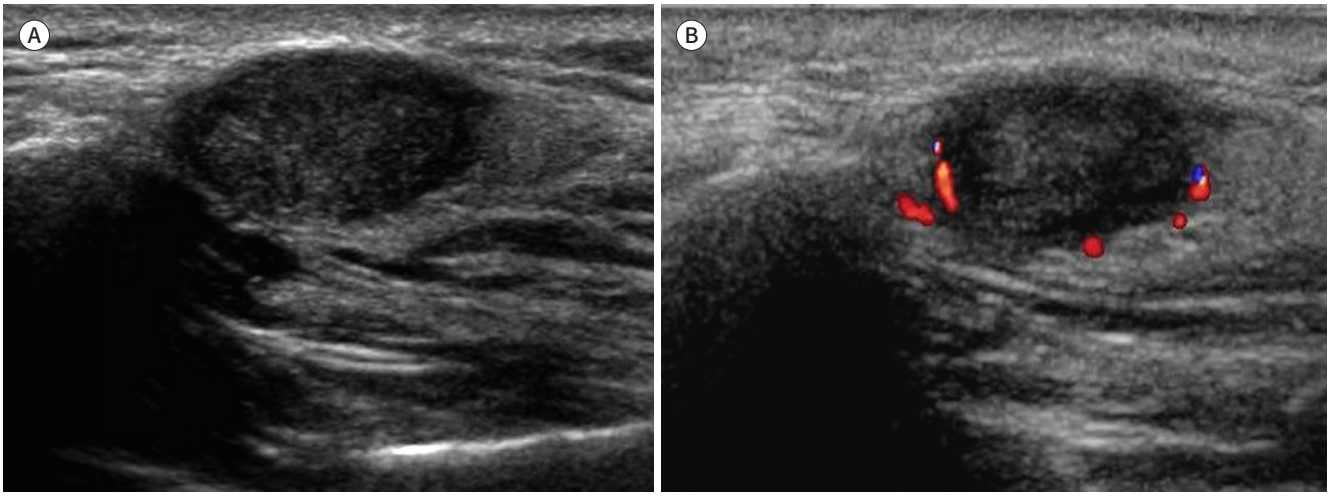

Fig. 10. Carcinoma ex pleomorphic adenoma in a 69-year-old-man.
A. T1-weighted axial MRI shows a large lobulated mass of the left parotid gland with intermediate and slightly high signal intensities (arrow).
B. Fat-suppressed T2-weighted axial MRI shows heterogeneous low to high signal intensity of the mass (arrow).
C. Post-contrast fat-suppressed T1-weighted axial image shows heterogeneous strong enhancement of the mass with tumor necrosis (arrow). Tumor invasion is noted in the left masticator space and retromastoid soft tissue.

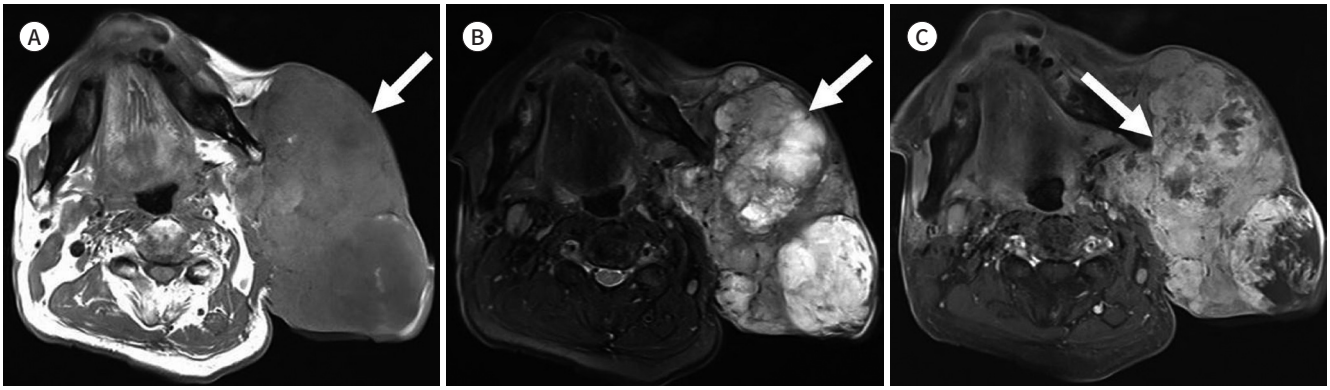

CONCLUSION

Various lesions of the scalp and face can occur from the skin to the skull with superficially palpable symptoms. Superficially palpable lesions of the scalp and face tend to be benign and small in size, but malignant lesions may be fast-growing large masses. Of the imaging modalities, US is especially useful for identifying the origin of lesions and for the evaluation of small and superficial lesions. CT and MRI studies provide superior soft tissue resolution and reveal characteristic soft tissue features. A knowledge of the common lesions of the scalp and face and use of the appropriate imaging examinations will be helpful in the diagnosis and treatment.

Conflicts of Interest

The authors have no potential conflicts of interest to disclose.

REFERENCES

1. El-Naggar AK, Chan JK, Grandis JR, Takata T, Slootweg PJ. *WHO classification of head and neck tumours*, 4th ed. Lyon: IARC press, 2017
2. Eskey CJ, Robson CD, Weber AL. Imaging of benign and malignant soft tissue tumors of the neck. *Radiol Clin North Am* 2000;38:1091-1104
3. Beaman FD, Kransdorf MJ, Andrews TR, Murphey MD, Arcara LK, Keeling JH. Superficial soft-tissue masses: analysis, diagnosis, and differential considerations. *Radiographics* 2007;27:509-523
4. Huang CC, Ko SF, Huang HY, Ng SH, Lee TY, Lee YW, et al. Epidermal cysts in the superficial soft tissue: sonographic features with an emphasis on the pseudotestis pattern. *J Ultrasound Med* 2011;30:11-17
5. Nigam JS, Bharti JN, Nair V, Gargade CB, Deshpande AH, Dey B, et al. Epidermal cysts: a clinicopathological analysis with emphasis on unusual findings. *Int J Trichology* 2017;9:108-112
6. Taira N, Aogi K, Ohsumi S, Takashima S, Kawamura S, Nishimura R. Epidermal inclusion cyst of the breast. *Breast Cancer* 2007;14:434-437
7. Fisher AR, Mason PH, Wagenhals KS. Ruptured plantar epidermal inclusion cyst. *AJR Am J Roentgenol* 1998;171:1709-1710
8. Hong SH, Chung HW, Choi JY, Koh YH, Choi JA, Kang HS. MRI findings of subcutaneous epidermal cysts: emphasis on the presence of rupture. *AJR Am J Roentgenol* 2006;186:961-966
9. Stone MS. Cysts. In Bolognia JL, Schaffer JV, Cerroni L, eds. *Dermatology*, 4th ed. Philadelphia: Elsevier, 2018:1917-1929
10. Jin W, Ryu KN, Kim GY, Kim HC, Lee JH, Park JS. Sonographic findings of ruptured epidermal inclusion cysts in superficial soft tissue: emphasis on shapes, pericystic changes, and pericystic vascularity. *J Ultrasound Med* 2008;27:171-176
11. Yasumoto M, Shibuya H, Gomi N, Kasuga T. Ultrasonographic appearance of dermoid and epidermoid cysts in the head and neck. *J Clin Ultrasound* 1991;19:455-461
12. Yuan WH, Hsu HC, Lai YC, Chou YH, Li AF. Differences in sonographic features of ruptured and unruptured epidermal cysts. *J Ultrasound Med* 2012;31:265-272
13. Kim HK, Kim SM, Lee SH, Racadio JM, Shin MJ. Subcutaneous epidermal inclusion cysts: ultrasound (US) and MR imaging findings. *Skeletal Radiol* 2011;40:1415-1419
14. Langer JE, Ramchandani P, Siegelman ES, Banner MP. Epidermoid cysts of the testicle: sonographic and MR imaging features. *AJR Am J Roentgenol* 1999;173:1295-1299
15. Shibata T, Hatori M, Satoh T, Ehara S, Kokubun S. Magnetic resonance imaging features of epidermoid cyst in the extremities. *Arch Orthop Trauma Surg* 2003;123:239-241
16. Alsaad KO, Obaidat NA, Ghazarian D. Skin adnexal neoplasms-part 1: an approach to tumours of the pilosebaceous unit. *J Clin Pathol* 2007;60:129-144
17. Haller JO, Kassner EG, Ostrowitz A, Kottmeler PK, Perfschuk LP. Pilomatrixoma (calcifying epithelioma of Malherbe): radiographic features. *Radiology* 1977;123:151-153
18. Garioni E, Danesino GM, Madonia L. Pilomatricoma: sonographic features. *J Ultrasound* 2008;11:76-78
19. Lin SF, Xu SH, Xie ZL. Calcifying epithelioma of malherbe (Pilomatrixoma): clinical and sonographic features. *J Clin Ultrasound* 2018;46:3-7
20. Wassef M, Blei F, Adams D, Alomari A, Baselga E, Berenstein A, et al. Vascular anomalies classification: recommendations from the international society for the study of vascular anomalies. *Pediatrics* 2015;136:e203-e214
21. George A, Mani V, Noufal A. Update on the classification of hemangioma. *J Oral Maxillofac Pathol* 2014;18:S117-S120
22. Buckmiller LM, Richter GT, Suen JY. Diagnosis and management of hemangiomas and vascular malformations of the head and neck. *Oral Dis* 2010;16:405-418
23. Griauzde J, Srinivasan A. Imaging of vascular lesions of the head and neck. *Radiol Clin North Am* 2015;53:197-213
24. Baer AH, Parmar HA, DiPietro MA, Kasten SJ, Mukherji SK. Hemangiomas and vascular malformations of the head and neck: a simplified approach. *Neuroimaging Clin N Am* 2011;21:641-658
25. Mittal MK, Malik A, Sureka B, Thukral BB. Cystic masses of neck: a pictorial review. *Indian J Radiol Imaging* 2012;22:334-343

26. Adams A, Mankad K, Offiah C, Childs L. Branchial cleft anomalies: a pictorial review of embryological development and spectrum of imaging findings. *Insights Imaging* 2016;7:69-76
27. Brown RE, Harave S. Diagnostic imaging of benign and malignant neck masses in children-a pictorial review. *Quant Imaging Med Surg* 2016;6:591-604
28. Cappabianca S, Colella G, Pezzullo MG, Russo A, Iaselli F, Brunese L, et al. Lipomatous lesions of the head and neck region: imaging findings in comparison with histological type. *Radiol Med* 2008;113:758-770
29. Bancroft LW, Kransdorf MJ, Peterson JJ, O'Connor MI. Benign fatty tumors: classification, clinical course, imaging appearance, and treatment. *Skeletal Radiol* 2006;35:719-733
30. Lloret I, Server A, Taksdal I. Calvarial lesions: a radiological approach to diagnosis. *Acta Radiol* 2009;50:531-542
31. Colas L, Caron S, Cotten A. Skull vault lesions: a review. *AJR Am J Roentgenol* 2015;205:840-847
32. Garfinkle J, Melançon D, Cortes M, Tampieri D. Imaging pattern of calvarial lesions in adults. *Skeletal Radiol* 2011;40:1261-1273
33. Yalçin O, Yildirim T, Kizilkiliç O, Hürcan CE, Koç Z, Aydin V, et al. CT and MRI findings in calvarial non-infectious lesions. *Diagn Interv Radiol* 2007;13:68-74
34. Thoeny HC. Imaging of salivary gland tumours. *Cancer Imaging* 2007;30:52-62
35. Lee YY, Wong KT, King AD, Ahuja AT. Imaging of salivary gland tumours. *Eur J Radiol* 2008;66:419-436
36. Cantisani V, David E, Sidhu PS, Sacconi B, Greco A, Pandolfi F, et al. Parotid gland lesions: multiparametric ultrasound and MRI features. *Ultraschall Med* 2016;37:454-471
37. Barton F, Branstetter IV. Mucoepidermoid carcinoma, parotid. In Harnsberger HR, Glastonbury CM, Michel MA, Koch BL, eds. *Diagnostic imaging-head and neck*. Salt Lake: Amirsys Inc, 2005
38. Som PM, Brandwein MS. *Salivary glands: anatomy and pathology*. In Som PM, Curtin DC, eds. *Head and neck imaging*, 4th ed. St. Louis: Mosby, 2003:2005-2133

두피 및 얼굴의 표재성 촉지병변: 임상화보

김형섭 · 안진경* · 우정주 · 윤라경

두피 및 얼굴의 표재성 촉지병변은 임상에서 흔히 볼 수 있다. 이들은 대체로 작고 양성인 경우가 많아 임상 증상에 따라 간단히 처리되기도 한다. 그러나 적절한 치료를 위해 정확한 병변의 종류와 위치를 파악하기 위한 영상검사가 종종 시행되고 있다. 초음파는 작은 표재성 병변을 분석하는 데 일차적이고 결정적인 검사로 유용하다. 컴퓨터단층촬영과 자기공명영상은 특징적인 연조직 소견을 나타내고 우수한 해상도를 제공한다. 본 임상화보에서는 표재성 촉지병변의 증상으로 나타나는 두피와 얼굴의 다양한 병변들과 이들의 영상소견을 설명하고자 한다.

을지대학교 노원을지병원 영상의학과